

Collision scenarios and probabilistic collision damage

A.J. Brown*

*Department of Aerospace and Ocean Engineering, Virginia Polytechnic Institute and State University,
Blacksburg, VA 24061, USA*

Received 15 April 2001; accepted 15 December 2001

Abstract

This paper examines the influence of collision scenario random variables on the extent of predicted damage in ship collisions. Struck and striking ship speed, collision angle, striking ship type and striking ship displacement are treated as independent random variables. Other striking ship characteristics are treated as dependent variables derived from the independent variables based on relationships developed from worldwide ship data. A Simplified Collision Model (SIMCOL) is used to assess the sensitivity of probabilistic damage extent to these variables. SIMCOL applies the scenario variables directly in a time-stepping simultaneous solution of internal (structural) and external (ship) problems. During the simultaneous solution SIMCOL also calculates struck ship absorbed energy in the longitudinal and transverse directions. These results are compared to absorbed energy estimates based on uncoupled external dynamics only. The necessity and effectiveness of this approach is examined. © 2002 Published by Elsevier Science Ltd.

Keywords: Ship collision; Ship damage; Probabilistic; Collision scenario; Collision model

1. Introduction

The serious consequences of ship collisions necessitate the development of regulations and requirements for the sub-division and structural design of ships to minimize damage, reduce environmental pollution, and improve safety. The Society of Naval Architects and Marine Engineers (SNAME) Ad Hoc Panel #6 was established to study the effect of structural design on the extent of damage in ship

*Tel.: +1-540-231-4950; fax: +1-540-231-9632.

E-mail address: brown@aoe.vt.edu (A.J. Brown).

collision and grounding. SNAME and the Ship Structure Committee (SSC) sponsor research under this panel as reported by Sirkar et al. [1], Crake [2], Rawson et al. [3], Chen [4], and Brown et al. [5]. A Simplified Collision Model (SIMCOL) was developed as part of this research. It is used in a Monte Carlo simulation as described by Brown and Amrozowicz [6] to predict probabilistic damage. Preliminary results from this research are presented in this paper.

The collection of collision and collision scenario data is an essential element in this development. Collision data are required for two purposes:

- collision model validation; and
- definition of probabilistic collision scenarios.

These two data requirements are very different. This paper considers only the analysis of data to define probabilistic collision scenarios.

Thousands of cases are required to develop probabilistic descriptions of possible collision scenarios. For a given struck ship design, the collision scenario is defined probabilistically using random variables. Collision angle, strike location, and ship speed data must be collected from actual collision events or developed using a ship encounter model. Striking ship data may come from actual collision events, local or regional models or worldwide ship characteristics.

This paper provides a preliminary set of probabilities, probability density functions and equations required to generate specific collision scenarios in a Monte Carlo simulation using SIMCOL. It assesses the sensitivity of structural damage (penetration and length) to each of these independent variables applied in 10,000 collision scenarios with each of four different struck ships, and it assesses the necessity of solving the internal damage problem simultaneously with the external ship dynamics.

2. SIMCOL

SIMCOL uses a time-domain simultaneous solution of external ship dynamics and internal deformation mechanics similar to that originally proposed by Hutchison [7].

SIMCOL Version 0.0 was developed as part of the work of SNAME Ad Hoc Panel #3 [1]. Based on further research, test runs and the need to make the model sensitive to a broader range of design and scenario variables, improvements were made progressively by SNAME Ad Hoc Panel #6. A sweeping segment method was added to the model in SIMCOL Version 1.0 to improve the calculation of damage volume and the direction of damage forces. Models from Rosenblatt [8] and McDermott [9] were applied in Version 1.1 assuming rigid web frames. In Version 2.0, the lateral deformation of web frames was included. In Version 2.1, the vertical extent of the striking ship bow is considered. Table 1 summarizes the evolution of SIMCOL over the last five years. Version 2.1 is used for the research presented in this paper and is described in the following sections.

Table 1
SIMCOL evolution

| Version | 0.1 | 1.0 | 1.1 | 2.0 | 2.1 |
|---------------------------------------|---|--|--|--|---------------------------------|
| Simulation | Simulation in time domain | | | | |
| External model | Three degrees of freedom (Hutchison and Crake) | | | | |
| Horizontal members | Minorsky mechanism as revalidated by Reardon and Sprung | | | | |
| | Crake's model | Sweeping segment method to calculate damaged area and resulting forces and moments | | | |
| Vertical members w/o rupture of plate | Jones and Van Mater | | McDermott/Rosenblatt study methods | | |
| Internal model | Crake's model (Jones) | Van Mater's extension of Jones | Does not consider deformation of webs, friction force and the force to propagate yielding zone | Considers deformation of webs, friction force and the force to propagate yielding zone | Striking bow with limited depth |
| Vertical members w/o ruptured plate | Neglected | | | Minorsky method for calculating absorbed energy due to longitudinal motion | |

2.1. SIMCOL External Dynamics Sub-Model

Fig. 1 shows the SIMCOL simulation process. The Internal Sub-Model performs Steps 2 and 3 in this process. It calculates internal deformation due to the relative motion of the two ships, and the internal reaction forces resulting from this deformation. The External Sub-Model performs Steps 1 and 4 in this process. A summary of the External Sub-Model is provided in this section.

The External Dynamics Sub-Model uses a global coordinate system shown in Fig. 2. Its origin is at the initial ($t = 0$) center of gravity of the struck ship with the x -axis towards the bow of the struck ship. The initial locations and orientations of the struck and striking ships in the global coordinate system are:

$$\begin{aligned}
 x_{1,0} &= 0, & y_{1,0} &= 0, & \theta_{1,0} &= 0, \\
 x_{2,0} &= -l_0 + \frac{L_{BP2}}{2} \cos \phi_0, \\
 y_{2,0} &= \frac{B_1}{2} + \frac{L_{BP2}}{2} \sin \phi_0, \\
 \theta_{2,0} &= \phi_0 - \pi,
 \end{aligned}
 \tag{1}$$

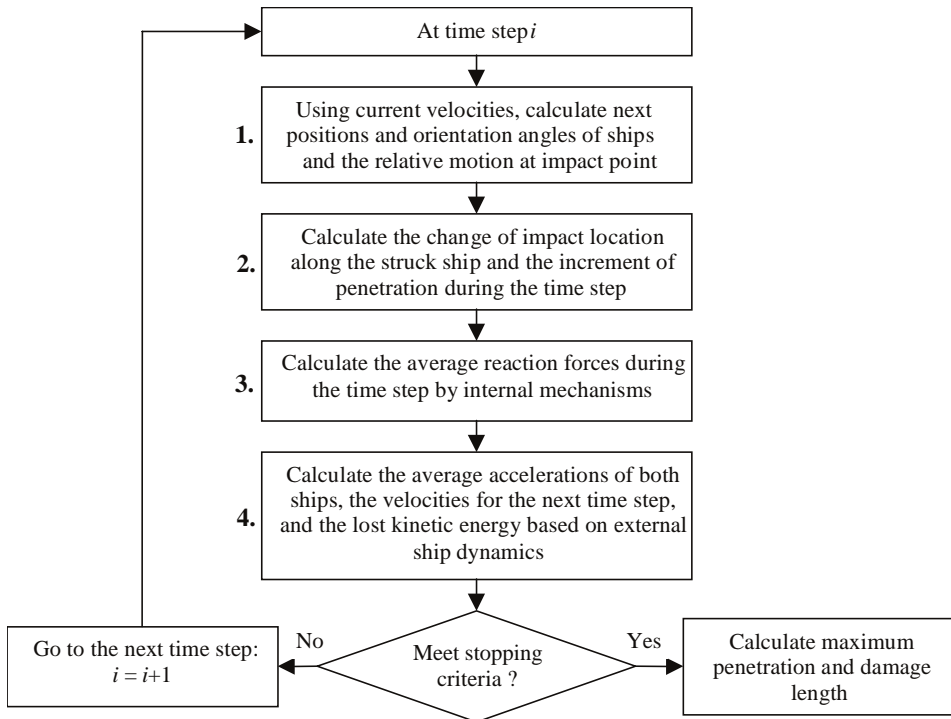


Fig. 1. SIMCOL simulation process.

where x_1, y_1 are the center of gravity of the struck ship (m), θ_1 the heading of the struck ship ($^\circ$), x_2, y_2 the center of gravity of the striking ship (m), θ_2 the heading of the striking ship ($^\circ$), L_{BP2} the LBP of the striking ship (m), B_1 the breadth of the struck ship (m), and ϕ the collision angle ($^\circ$).

A local damage coordinate system, $\xi-\eta$, is established on the struck ship to calculate relative movement and collision forces. The origin of this system is set at midship on the shell plate of the damaged side of the struck ship. Axes ξ and η point aft and inboard relative to the struck ship. Local coordinate systems are also established at the centers of gravity of both struck and striking ships. Forces and moments in the local systems are transformed to the global $x-y$ system for solution of the ship dynamics.

Considering the symmetry of the ships, and with the center of gravity of the ships assumed at midship, the local system added mass tensor for each ship is

$$\mathbf{A}_s = \begin{bmatrix} a_{11} & 0 & 0 \\ 0 & a_{22} & 0 \\ 0 & 0 & a_{33} \end{bmatrix}, \quad (2)$$

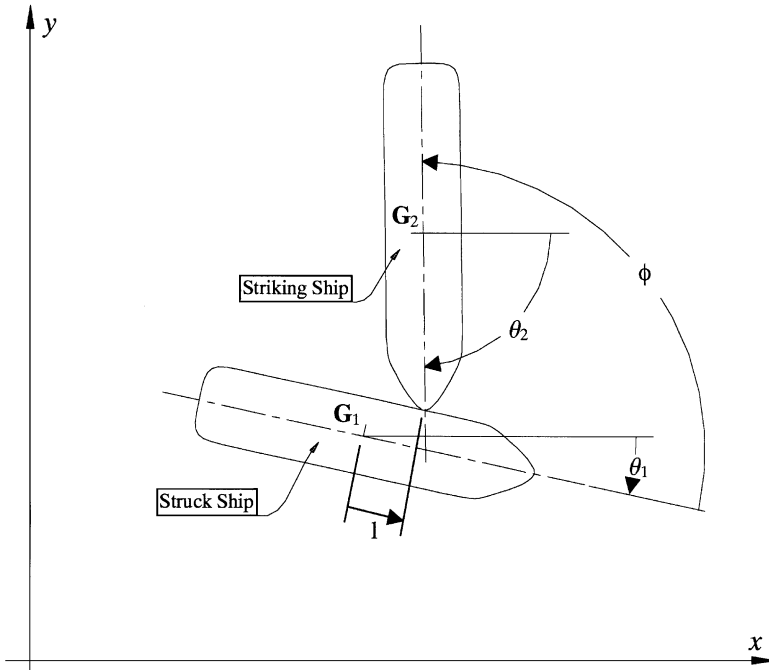


Fig. 2. SIMCOL global coordinate system.

where a_{11} is the added mass in the surge direction (kg), a_{22} the added mass in the sway direction (kg), and a_{33} the yaw added mass moment of inertia (kg m^2).

Average added mass values vary with the duration of the collision impact. Mid-range values are typically used. The added mass tensor is transformed in accordance with the orientation of each ship to the global coordinate system. The transformed tensor, \mathbf{A}_θ , for each ship is:

$$\mathbf{A}_\theta = \begin{bmatrix} a_{11} \cos^2 \theta + a_{22} \sin^2 \theta & (a_{11} - a_{22}) \cos \theta \sin \theta & 0 \\ (a_{11} - a_{22}) \cos \theta \sin \theta & a_{11} \sin^2 \theta + a_{22} \cos^2 \theta & 0 \\ 0 & 0 & a_{33} \end{bmatrix}. \tag{3}$$

The mass for each ship is represented by a tensor:

$$\mathbf{M}_{\text{ship}} = \begin{bmatrix} m_s & 0 & 0 \\ 0 & m_s & 0 \\ 0 & 0 & I_{s33} \end{bmatrix}, \tag{4}$$

where m_s is the mass of each ship (kg), and I_{s33} the yaw mass moment of inertia (kg m^2).

The virtual mass, \mathbf{M}_V , for each ship is then

$$\begin{aligned} \mathbf{M}_{V\theta} = \mathbf{M}_{\text{ship}} + \mathbf{A}_\theta &= \begin{bmatrix} m_{V11} & m_{V12} & 0 \\ m_{V21} & m_{V22} & 0 \\ 0 & 0 & I_{V33} \end{bmatrix} \\ &= \begin{bmatrix} m_s + a_{11} \cos^2 \theta + a_{22} \sin^2 \theta & (a_{11} - a_{22}) \cos \theta \sin \theta & 0 \\ (a_{11} - a_{22}) \cos \theta \sin \theta & m_s + a_{11} \sin^2 \theta + a_{22} \cos^2 \theta & 0 \\ 0 & 0 & I_{s33} + a_{33} \end{bmatrix}. \end{aligned} \quad (5)$$

Referring to Fig. 1, Step 1, the velocities from the previous time step are applied to the ships to calculate their positions at the end of the current time step:

$$\mathbf{X}_{n+1} = \mathbf{X}_n + \mathbf{V}_{sn}\tau, \quad (6)$$

where \mathbf{X} is the location and orientation of ships in the global system, $\mathbf{X} = \{x, y, \theta\}^T$, \mathbf{V}_{sn} the ship velocity, $\mathbf{V}_s = \{u, v, \omega\}^T$, and τ the time step (s).

In Steps 2 and 3, the Internal Model calculates the compatible deformation, and the average forces and moments generated by this deformation over the time step. In Step 4, these forces and moments are applied to each ship. The new acceleration for each ship is

$$\mathbf{V}'_s = \frac{\mathbf{F}}{\mathbf{M}_{Vg}}, \quad (7)$$

where \mathbf{F} is the forces exerted on the ships in the global system, $\mathbf{F} = \{F_x, F_y, M\}^T$, and \mathbf{V}'_s the ship acceleration, $\mathbf{V}'_s = \{u', v', \omega'\}^T$ and

$$\begin{aligned} u' &= \frac{F_x m_{V22} - F_y m_{V12}}{m_{V11} m_{V22} - m_{V12}^2}, \\ v' &= \frac{F_y m_{V11} - F_x m_{V12}}{m_{V11} m_{V22} - m_{V12}^2}, \\ \omega' &= \frac{M}{I_{V33}}. \end{aligned} \quad (8)$$

The new velocity for each ship at the end of the time step is then

$$\mathbf{V}_{s,n+1} = \mathbf{V}_{s,n} + \mathbf{V}'_s \tau. \quad (9)$$

2.2. SIMCOL Internal Sub-Model

The Internal Sub-Model calculates the struck ship deformation resulting from the ships' relative motion, and calculates the average internal forces and moments generated by this deformation over the time step. Refer to Fig. 1, Steps 2 and 3. The Internal Sub-Model determines reacting forces from side and bulkhead (vertical) structures using specific component deformation mechanisms including: membrane tension; shell rupture; web frame bending; shear and compression; force required to propagate the yielded zone; and friction. It determines absorbed energy and forces

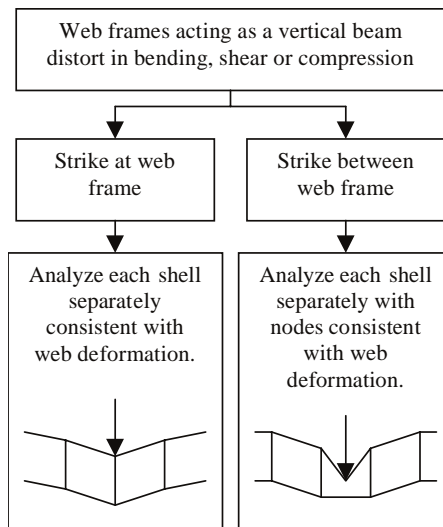


Fig. 3. Web deformation in SIMCOL 2.0 [8].

from the crushing and tearing of decks, bottoms and stringers (horizontal structures) using the Minorsky [10] correlation as modified by Reardon and Sprung [11]. Total forces are the sum of these two components. In SIMCOL Version 2.1, the striking ship bow is assumed to be rigid and wedge-shaped with upper and lower extents determined by the bow height of the striking ship and the relative drafts of the two ships. Deformation is only considered in the struck ship. The striking ship bow is assumed to be rigid.

Penetration of the struck ship begins with the side shell plating and webs (vertical structures). Fig. 3 illustrates the two basic types of strike determined by the strike location relative to the webs.

In this analysis:

- Plastic bending of shell plating is not considered. The contribution of plastic bending in the transverse deformation of longitudinally stiffened hull plates is negligible. The sample calculation sheets in Rosenblatt [8] support this argument. In six test cases, the energy absorbed in plastic bending never exceeds 0.55% of the total absorbed energy when the cargo boundary is ruptured. It is a good assumption that the plastic membrane tension phase starts from the beginning of collision penetration and is the primary shell energy-absorption mechanism.
- Rupture of stiffened hull plates starting in the stiffeners is not considered. This mechanism is unlikely for most structures except for flat-bar stiffened plates. It is a standard practice to use angles or bulbs instead of flat bar for longitudinal stiffeners of side shell and longitudinal bulkheads, therefore, this option is not considered in SIMCOL.

- Web frames do not yield or buckle before plates load in membrane tension. McDermott [9] demonstrates that this mechanism is unlikely and does not contribute significantly to absorbed energy in any case. This mechanism requires very weak web frames that would not be sufficient to satisfy normal sea and operational loads.

SIMCOL Version 1.1 assumes that flanking web frames are rigid. Version 2.0 and subsequent versions used for this paper consider the transverse deformation of webs. In a right-angle collision case, Eq. (10) gives the total plastic energy absorbed in membrane tension in time step n . This assumes that the plate is not ruptured, that flanking webs do not deflect in the longitudinal direction, and that compression in the side shell caused by longitudinal bending of the ship hull girder is small:

$$E_n = T_m e_m,$$

$$T_m = \sigma_m t B_e, (10)$$

where E_n is the plastic energy absorbed by side shell or longitudinal bulkhead (J), T_m the membrane tension (N), σ_m the yield stress of side shell or bulkhead adjusted for strain rate (Pa), e_m the total elongation of shell or bulkhead structure between damaged webs, t the smeared thickness of side shell or bulkhead plating and stiffeners (m), and B_e the effective breadth (height) of side shell or bulkhead (m).

Fig. 4 illustrates the membrane geometry for calculation of elongation. e_1 and e_2 are the elongation of legs L_1 and L_2 , respectively:

$$e_i = \sqrt{L_i^2 + w^2} - L_i \cong \frac{w^2}{2L_i},$$

$$e_t = e_1 + e_2 = \frac{L_d}{2L_1 L_2} w^2 \tag{11}$$

and L_d is the distance between adjacent webs (m), and w_n the transverse deflection at time step n (m).

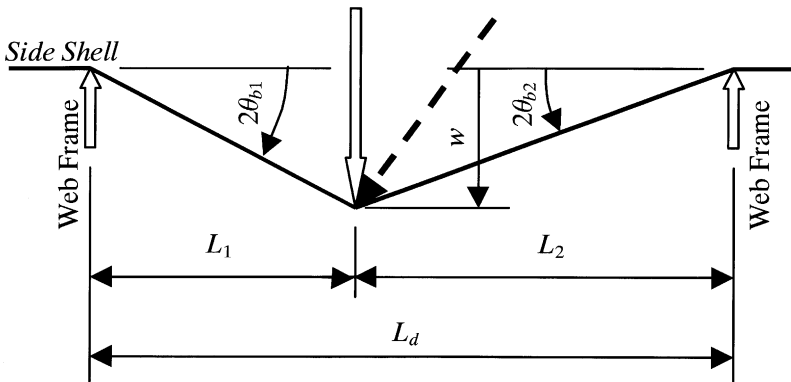


Fig. 4. Membrane geometry [8].

Side shell rupture due to membrane tension is predicted using the following criteria:

- the strain in the side shell reaches the rupture strain, ϵ_r , taken as 10% in ABS steel; or
- the bending angle at a support reaches the critical value as defined in the following equation [8]:

$$\epsilon_m = \frac{4}{3} \frac{\sigma_m}{\sigma_u - \sigma_m \cos \theta_c} \sin \theta_c \tan \theta_c = 1.5D, \tag{12}$$

where, ϵ_m is the maximum bending and membrane-tension strain to rupture, σ_m the membrane-tension in-plate stress (MPa), σ_u the ultimate stress of the plate (MPa), θ_c the critical bending angle, and D the tension test ductility.

The resistance of the membrane is only considered up to the point of rupture:

$$\begin{aligned} \epsilon_i &= \frac{e_i}{L_i} \leq \epsilon_r, \\ \theta_{bi} &= \frac{1}{2} \arctan \frac{w}{L_i} \cong \frac{w}{2L_i} \leq \theta_c, \end{aligned} \tag{13}$$

where ϵ_i is the strain in leg i , and θ_{bi} the bending angle of flanking web frames.

Since the striking bow normally has a generous radius, the bending angle at the impact location is not considered in the rupture criteria. From these equations, it is seen that only the strain and bending angle in the shorter leg need to be considered for right angle collisions. Based on material properties of ABS steel, the critical bending angles θ_c from Eq. (12) are 19.896°, 17.318° or 16.812° for MS, H32 or H36 grades, respectively. Once either of the rupture criteria is reached, the side shell or longitudinal bulkhead is considered ruptured and does not continue to contribute to the reacting force.

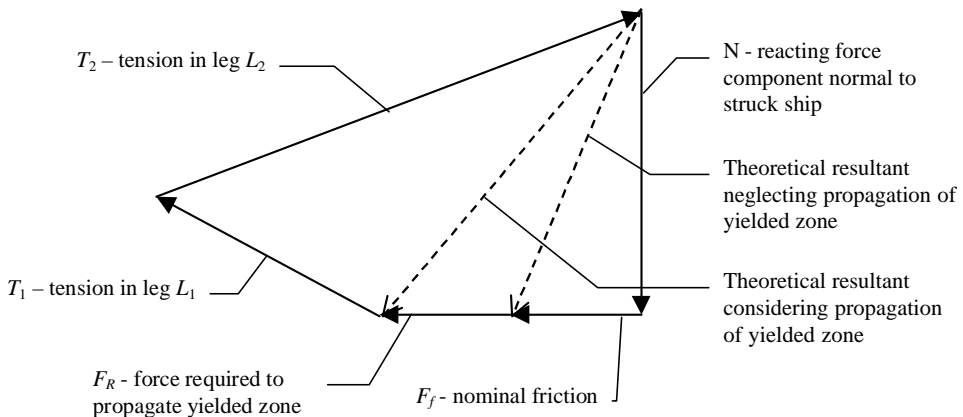


Fig. 5. Oblique collision force diagram [9].

For collisions at an oblique angle, the membrane tension is only fully developed in the leg behind the strike, L_2 in Fig. 4. This is demonstrated in the force diagram shown in Fig. 5, where T_1 is much smaller than T_2 . It is also assumed that all the strain developed from membrane tension is behind the striking point. Therefore, the first rupture criterion in Eq. (13) becomes

$$\varepsilon_b = \frac{e_t}{L_b} \leq \varepsilon_r, \quad (14)$$

where ε_b and L_b represent the strain and length of the leg behind the striking. In Fig. 4, they are ε_2 and L_2 , respectively.

In SIMCOL Version 2.0 and later, transverse deformation of web frames is also considered. Web failure modes include bending, shear, and compression. Web frames allow transverse deformation while keeping their longitudinal locations. The resisting force is assumed constant at a distorted flanking web frame, and the transverse deformation of the web frame is assumed uniform from top to bottom. The magnitude of this force is its maximum elastic capacity. From Fig. 5, the applied force on a rigid flanking web frame is

$$P_i = T_i \frac{w}{L_i}, \quad (15)$$

where P_i and T_i are referred to the particular leg L_i . If the applied force, P_i , is greater than the maximum elastic capacity of the flanking web, P_{wf} , the particular web frame is deformed as shown in Fig. 6.

The change of angle, γ_c , at the distorted web is then

$$\gamma_{ci} \cong \frac{P_{wf}}{T_i}. \quad (16)$$

Rosenblatt [8] proposed an approach to determine whether P_i exceeds the capacity P_{wf} , and to estimate the value of P_{wf} . First, the allowable bending moment and shear force of the web frame at each support, the crushing load of the web, and the buckling force of supporting struts are calculated. Then, the load P_i is applied to the web frame, and the induced moments, shear forces and compression of the web frame and struts are calculated, considering the web frame as a beam with clamped ends. The ratios of the induced loads to the allowable loads are determined using

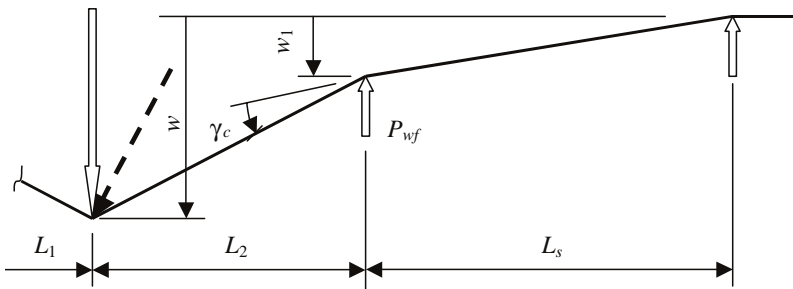


Fig. 6. Deflection and forces in web frames [8].

Eq. (17). If the maximum ratio, R_m , is greater than unity, the load, P , exceeds the capacity, and the web frame deforms. R_m is also used to estimate the number of distorted web frames:

$$R_m = \frac{P}{P_{wf}}. \quad (17)$$

The deflection at the outermost distorted web is

$$w_n = \frac{L_s}{L_i + nL_s} \left\{ w - \gamma_{c2} \left[nL_i + \frac{1}{2}(n-1)nL_s \right] \right\}, \quad (18)$$

where n is the number of deformed web frames on L_i side and L_s the web frame spacing (m).

The deflection at other deformed web frames is

$$w_j = (n-j+1)w_n + \frac{1}{2}(n-j)(n-j+1)\gamma_{c2}L_s, \quad (19)$$

where j is the number of webs counted from the striking point. The elongation in adjacent webs is

$$e_j = \sqrt{(w_j - w_{j+1})^2 + L_s^2} - L_s \quad (20)$$

and the elongation in the struck web is

$$e_{0i} = \sqrt{(w - w_1)^2 + L_i^2} - L_i. \quad (21)$$

With these elongation and deformation results, the rupture criteria given in Eqs. (13) and (14) are applied to all deformed webs. The total elongation on the L_i side is

$$e_{ti} = e_{0i} + \sum_{j=1}^n e_{ji} \quad (22)$$

and the energy absorbed in membrane tension and web deformation is

$$E_i = T_i e_{ti} + P_{wf} \sum_{j=1}^n w_{ji}. \quad (23)$$

For right angle collisions, T_i always equals T_m as calculated in Eq. (10). In oblique angle collisions, T_i equals T_m if L_i is on the side behind the strike. Based on experimental data, Rosenblatt [8] suggests using $1/2T_m$ ahead of the strike and this is used in SIMCOL 2.1.

For double hull ships, if the web frames are distorted because of bending, shearing and buckling of supporting struts, the deformed web frames push the inner skin into membrane tension as shown in Fig. 3, and the right angle collision mechanism is applied to the inner hull. Inner skin integrity is checked using Eqs. (13) and (14), and the energy absorbed in inner skin membrane tension is calculated using Eq. (10).

In the simulation, the energy absorbed in membrane tension and web deformation during the time step is

$$\Delta KE_n = (E_{1,n+1} + E_{2,n+1}) - (E_{1n} + E_{2,n}). \quad (24)$$

Considering the friction force, F_f , shown in Fig. 5, and assuming the dynamic coefficient of friction is a constant value of 0.15, the reacting forces and moments are:

$$\begin{aligned}\Delta KE_n &= N_n(w_{n+1} - w_n) + F_{fn}|l_{n+1} - l_n| = N[(w_{n+1} - w_n) + 0.15|l_{n+1} - l_n|], \\ F_{\eta n} &= N_n = \frac{(E_{1,n+1} + E_{2,n+1}) - (E_{1n} + E_{2n})}{(w_{n+1} - w_n) + 0.15|l_{n+1} - l_n|}, \\ F_{\xi n} &= F_f \frac{(l_{n+1} - l_n)}{|l_{n+1} - l_n|} = 0.15F_{\eta n} \frac{(l_{n+1} - l_n)}{|l_{n+1} - l_n|}, \\ M_n &= -F_{\xi n}d_n + F_{\eta n}l_n.\end{aligned}\quad (25)$$

In addition to the friction force, another longitudinal force, F_R , the force to propagate the yielding zone, is considered, as shown in Fig. 5. McDermott [9] provides an expression for this force:

$$F_R = \frac{\sigma_y d'}{R} \left[d' t_w \left(1 - \frac{\sigma_y R}{d' E} \right)^2 + t_f (b - t_w) \left(\frac{d' - 0.5 t_f}{d'} - \frac{\sigma_y R}{d' E} \right) \right], \quad (26)$$

where d' is the depth of side shell longitudinal stiffeners, R the radius of the striking bow, t_w the thickness of side shell stiffener webs, t_f the thickness of side shell stiffener flanges, b the width of side shell stiffener flanges, and E the modulus of elasticity, or

$$\begin{aligned}c_F &= \frac{F_R}{\sigma_y A_{\text{stiff}}}, \\ c_A &= \frac{A_{\text{stiff}}}{A_{\text{total}}}, \\ F_R &= c_F c_A \sigma_y t B,\end{aligned}\quad (27)$$

where c_F is the force coefficient, c_A the ratio of sectional areas, A_{stiff} the sectional area of stiffeners, and A_{total} the total sectional area of stiffeners and their attached plate.

The full implementation of Eq. (26) requires structural details that are not appropriate for a simplified analysis so Eq. (27) is used in this study. Based on a sampling of typical side shell scantlings, $c_F c_A$ is assumed to have a constant value of 0.025.

Since F_R also effects membrane tension energy, Eq. (25) becomes

$$\begin{aligned}\Delta KE_n &= F_{\eta n}[(w_{n+1} - w_n) + 0.15|l_{n+1} - l_n| + F_R(l_{n+1} - l_n)], \\ F_{\eta n} &= \frac{(E_{1,n+1} + E_{2,n+1}) - (E_{1n} + E_{2n}) - F_R(l_{n+1} - l_n)}{(w_{n+1} - w_n) + 0.15|l_{n+1} - l_n|}, \\ F_{\xi n} &= (F_R + 0.15F_{\eta n}) \frac{(l_{n+1} - l_n)}{|l_{n+1} - l_n|}, \\ M_n &= -F_{\xi n}d_n + F_{\eta n}l_n.\end{aligned}\quad (28)$$

The Internal Sub-Model determines absorbed energy and forces from the crushing and tearing of decks, bottoms and stringers (horizontal structures) in a simplified manner using the Minorsky [10] correlation as modified by Reardon and Sprung [11].

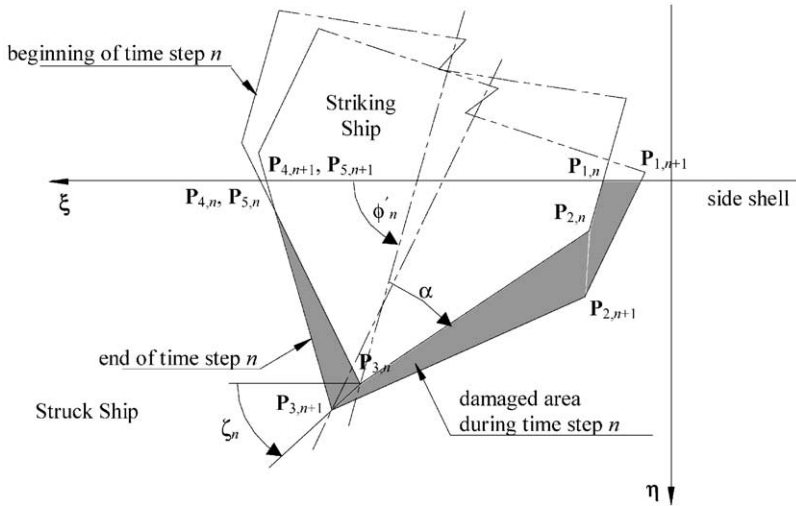


Fig. 7. Sweeping segment method.

V.U. Minorsky conducted the first and best known of the empirical collision studies based on actual data. His method relates the energy dissipated in a collision event to the volume of damaged structure. Actual collisions in which ship speeds, collision angle, and extents of damage are known were used to empirically determine a linear constant. This constant relates damage volume to energy dissipation. In the original analysis the collision is assumed to be totally inelastic, and motion is limited to a single degree of freedom. Under these assumptions, a closed form solution for damaged volume can be obtained. With additional degrees of freedom, a time-stepped solution must be used.

Step 2 in the collision simulation process calculates damaged area and volume in the struck ship given the relative motion of the two ships in a time step calculated in Step 1 by the External Sub-Model. Fig. 7 illustrates the geometry of the sweeping segment method used for this calculation in SIMCOL Version 2.1.

The intrusion portion of the bow is described with five nodes, as shown in Fig. 7. The shaded area in Fig. 7 shows the damaged area of decks and/or bottoms during the time step. Coordinates of the five nodes in the $\xi-\eta$ system at each time step are derived from the penetration and location of the impact, the collision angle, ϕ , and the half entrance angle, α , of the striking bow.

The damaged plating thickness t is the sum thickness of deck and/or bottom structures that are within the upper and lower extents of the striking bow. Given the damaged material volume, the Minorsky force is calculated based on the following assumptions:

- The resistant force acting on each out-sweeping segment is in the opposite direction of the average movement of the segment.
- The force exerted on the struck ship is in the direction of this average movement.

- The work of the resistant force is done over the distance of this average movement.
- The total force on each segment acts through the geometric center of the sweeping area.

The energy absorbed is then

$$\Delta KE_{1,n} = 47.1 \times 10^6 R_{T1,n} = 47.1 \times 10^6 A_{1,n} t, \quad (29)$$

where ΔKE is the kinetic energy absorbed by decks, bottoms and stringers (J), R_T the damaged volume of structural members (m^3), A the damaged area of the decks or bottoms swept by each bow segment (m^2), and t the total thickness of impacted decks or bottoms (m).

Forces and moments acting on other segments are calculated similarly. The total exerted force, \mathbf{F}_n , is the sum of the forces and moments on each segment:

$$\mathbf{F}_n = \sum_{i=1}^4 \{F_{\xi i,n}, F_{\eta i,n}, M_{i,n}\}. \quad (30)$$

These forces are added to the side shell, bulkhead and web forces. Internal forces and moments are calculated for the struck ship in the local coordinate system, i.e. the $\xi-\eta$ system, and converted to the global system. The forces and moments on the striking ship have the same magnitude and the opposite direction of those acting on the struck ship.

2.3. SIMCOL input data

SIMCOL requires two types of input data:

- data describing the struck ship; and
- data describing the collision scenario and striking ship.

The struck ship data include: struck ship type (single hull or double hull); principal characteristics (LBP, B , D , T , Δ); transverse web spacing; description of primary sub-division (number and location of transverse bulkheads, number and location of longitudinal bulkheads including the side shell); smeared plate thickness of side shell, longitudinal bulkheads, decks, bottom; material grades of side shell, longitudinal bulkheads, decks, bottom; number, width, location, smeared thickness, and material of side stringers; side shell supports including decks, bottom, and struts; web material, thickness, stiffener spacing, supported length; and strut material, area, radius of gyration, and critical length.

The scenario data include: striking ship principal characteristics; striking ship bow half-entrance angle (HEA), speed of the struck ship; speed of the striking ship; impact point location; and collision angle.

3. Collision scenarios

The collision scenario is described using random variables. Two primary data sources are used to determine the probabilities and probability density functions necessary to define these random variables:

- Sandia Report [12]; and
- Lloyd's Worldwide Ship data [13].

The Sandia Report considers collision data from four sources:

- Lloyd's Casualty Data for 1973–1993—contains 30,000 incident reports of which 1947 were ship-to-ship collision events, 702 of which occurred in ports. These data were used primarily to estimate the probability and geographical location of collisions and fires that could harm nuclear flasks. It did not include specific scenario and technical data. It is not directly applicable to collision scenarios.
- ORI Analysis [14]—includes a summary of data from cargo vessel accidents in 1974 and 1975 for 78,000 transits of ships over 5000 gross tons. Most of this data is from the USCG Commercial Vessel Casualty File. It includes 216 collisions for ships in US waters or US ships in international waters. Eight collisions of tankers and cargo ships and other tanker accidents from the ECO World Tanker Accident file are also included. This totals 1122 cargo ship accidents. One hundred and fifteen are struck cargo ship collisions with more than 90% of these in inland and coastal waters. The study addresses the probability of various accident types.
- ORI Analysis [15]—this study uses the same data as the ORI (1980) Study. It includes the probability of striking ship displacement, speed, collision angle and collision location for struck cargo ship collisions.
- Engineering Computer Optecnomics, Inc. World Fleet Data [14].

Applicable subsets of this data are described here. In this paper, pdfs generated from this data are used to develop 10,000 collision cases that are applied to four struck tanker designs, for a total of 40,000 SIMCOL runs. SIMCOL calculates damage penetration, damage length, oil outflow and absorbed energy for each of these runs.

3.1. Collision event variables

Collision event variables are not expected to be fully independent, but their interdependence is difficult to quantify because of limited collision data. Fig. 8 provides a framework for defining the relationship of scenario variables. Available data are incomplete to fully quantify this relationship. Strike location must often be inferred from the damage description because reliable records of the precise location are not available. Ship headings and speeds prior to the collision are often included in accident reports, but collision angle and ship speed at the moment of collision are frequently not included or only estimated and described imprecisely.

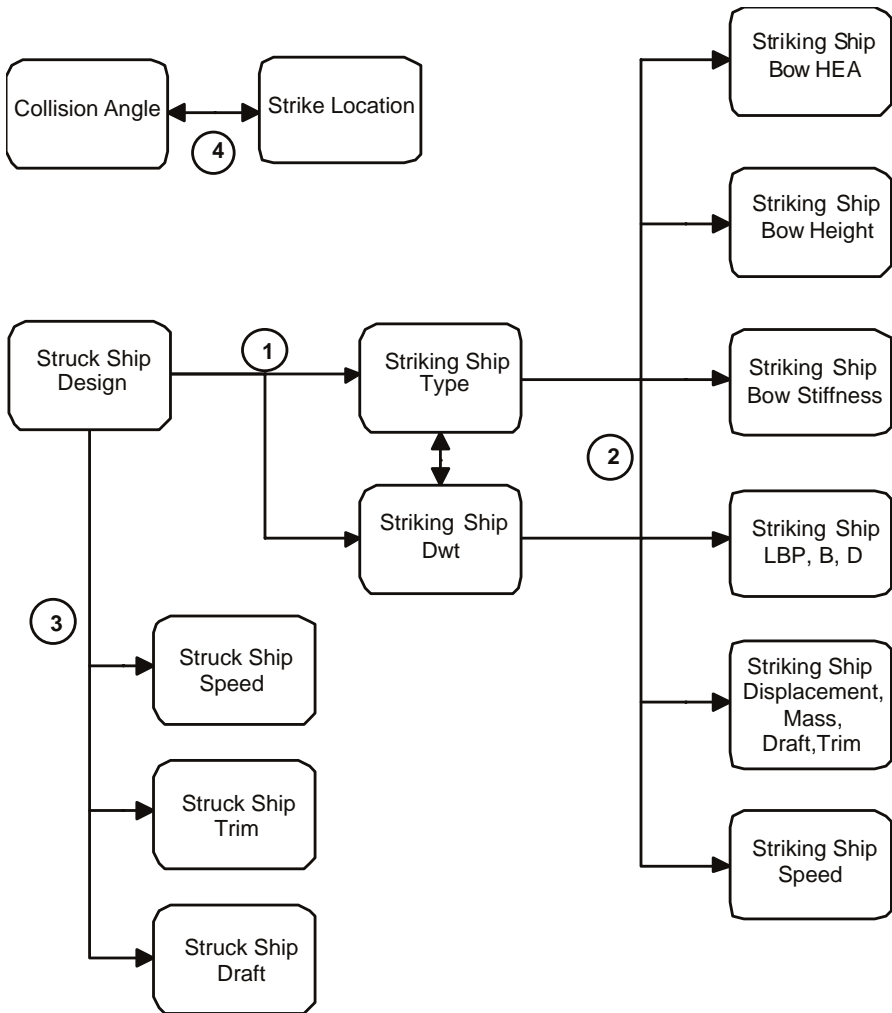


Fig. 8. Collision event variables.

3.2. Striking ship type and displacement

Fig. 9 provides probabilities of the struck ship encountering specific ship types. These probabilities are based on the fraction of each ship type in the worldwide ship population in 1993. Each of the general types includes a number of more specific types:

- Tankers—includes crude and product tankers, ore/oil carriers, LPG tankers, chemical tankers, LNG tankers, and oil/bulk/ore carriers.
- Bulk carriers—includes dry bulkers, ore carriers, fish carriers, coal carriers, bulk/timber carriers, cement carriers and wood chip carriers.

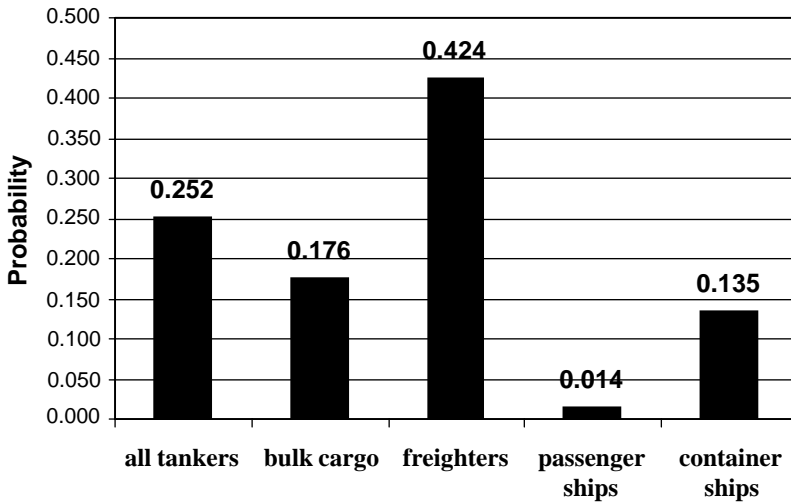


Fig. 9. Striking ship type probability.

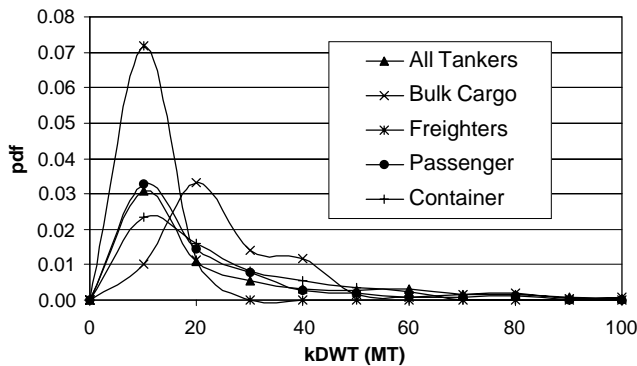


Fig. 10. Striking ship displacement, worldwide.

- Cargo vessels (break bulk/freighters)—includes general freighters and refrigerated freighters.
- Passenger—including passenger and combo passenger/cargo ships.
- Containerships—including containerships, car carriers, container/RO-ROs, ROROs, bulk/car carriers, and bulk/containerships.

It is likely that particular ships are more likely to meet ships of the same type since they travel the same routes, but this relationship could not be established with available data. Additional collision data must be obtained to establish this relationship.

Fig. 10 shows the worldwide distributions of displacement for these ship types. The distributions are significantly different and must be applied individually

Table 2
Striking ship type and displacement

| Ship type | Probability of encounter | Weibull α | Weibull β | Mean (kMT) | σ (kMT) |
|--------------|--------------------------|------------------|-----------------|------------|----------------|
| Tanker | 0.252 | 0.84 | 11.2 | 12.277 | 14.688 |
| Bulk carrier | 0.176 | 1.20 | 21.0 | 19.754 | 16.532 |
| Cargo | 0.424 | 2.00 | 11.0 | 9.748 | 5.096 |
| Passenger | 0.014 | 0.92 | 12.0 | 12.479 | 13.579 |
| Container | 0.135 | 0.67 | 15.0 | 19.836 | 30.52 |

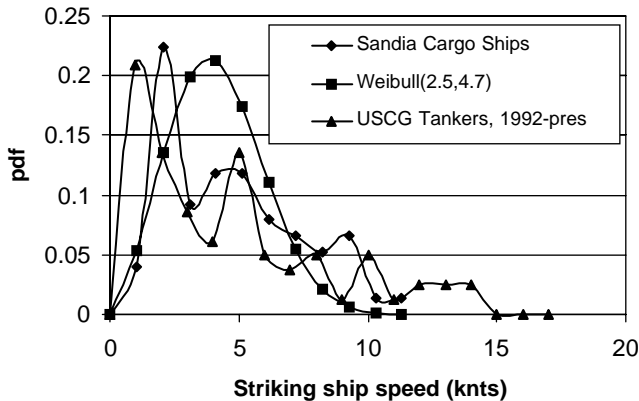


Fig. 11. Striking ship speed.

to each ship type. Weibull density function α and β values for each distribution are provided in Table 2.

Collision speed is the striking ship speed at the moment of collision. It is not necessarily related to service speed. It depends primarily on actions taken just prior to collision. Collision speed data are collected from actual collision events. Fig. 11 is a plot of data derived from the Sandia Report [12] and limited USCG tanker-collision data [16]. An approximate Weibull distribution ($\alpha = 2.2$, $\beta = 6.5$) is fit to this data. The mean of this distribution is substantially less than service speed (s), and indicates significant adjustment in speed prior to the actual collision event.

3.3. Striking ship principal characteristics

In this section, data and regression curves are presented for deriving striking ship HEA, length, beam, draft, and bow height from striking ship type and displacement.

Bow HEA is not a standard ship principal characteristic. A limited number of bow drawings were reviewed in the Sandia Study. Table 3 provides single values derived from this study for each type of ship. These values are used in this study.

Table 3
Striking ship characteristics ($y = Cx^a$ where x is displacement in ton)

| Ship type | LBP (m) | | Beam (m) | | Draft (m) | | Bow height (m) | | HEA |
|----------------|---------|-------|----------|-------|-----------|-------|----------------|-------|-----|
| | C | a | C | a | C | a | C | A | |
| Tanker | 7.47 | 0.318 | 1.15 | 0.321 | 0.574 | 0.297 | 0.671 | 0.320 | 38 |
| Bulk carrier | 6.6 | 0.332 | 0.96 | 0.336 | 0.547 | 0.303 | 1.31 | 0.261 | 20 |
| Freighter | 6.93 | 0.325 | 1.72 | 0.273 | 0.474 | 0.320 | 0.741 | 0.321 | 20 |
| Passenger ship | 8.22 | 0.299 | 1.97 | 0.256 | 0.889 | 0.210 | 1.13 | 0.258 | 17 |
| Container ship | 5.49 | 0.353 | 1.96 | 0.265 | 0.596 | 0.284 | 0.746 | 0.317 | 17 |

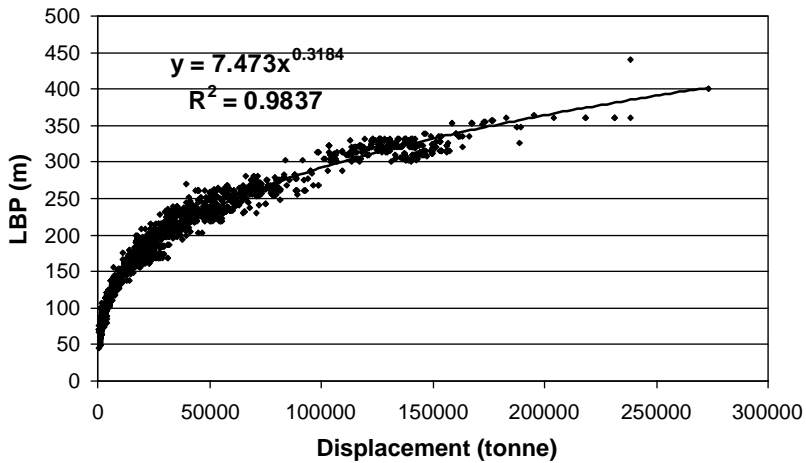


Fig. 12. Tankers length versus displacement.

Lloyd’s worldwide data [13] are used to specify the remaining principal characteristics as a function of ship type and displacement. Typical principal characteristic data are plotted in Fig. 12. These data are fit to a power function of the form: $y = Cx^a$, where x is displacement in ton. Table 3 provides values for coefficients and powers used in these equations.

3.4. Struck ship variables

Fig. 13 is a plot of struck ship speed derived from the USCG tanker collision data. The struck ship collision speed distribution is also very different from service speed. Struck ships are frequently moored or at anchor as is indicated by the significant pdf value at zero speed. An exponential distribution ($\alpha = 0.584$) is fit to this data. Full load displacement and draft with zero trim are assumed for the struck ship in this paper.

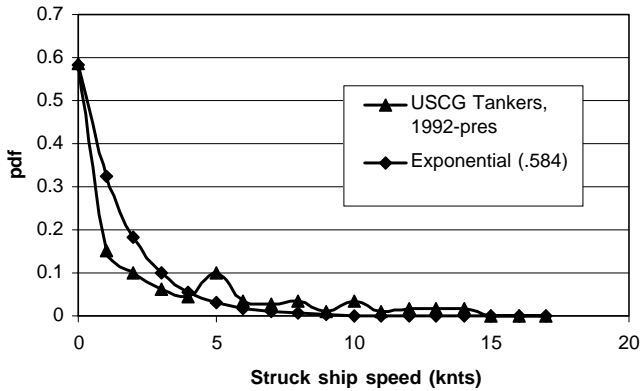


Fig. 13. Struck ship speed.

3.5. Remaining collision scenario variables

An approximate normal distribution ($\mu = 90^\circ$, $\sigma = 28.97^\circ$) is fit to collision angle data derived from the Sandia Report, and is used to select collision angle in the Monte Carlo simulation. At more oblique angles, there is a higher probability of ships passing each other or only striking a glancing blow. These cases are frequently not reported.

The current IMO pdf for longitudinal strike location specifies a constant value over the entire length of the struck ship, IMO [17]. The constant pdf was chosen for convenience and because of the limited available data. Fig. 14 shows a bar chart of the actual data used to develop the IMO pdf, IMO [18], and data gathered for cargo ships in the Sandia Study. These data do not indicate a constant pdf. The IMO data are from 56 of 200 significant tanker-collision events for which the strike location is known. The Sandia data indicate a somewhat higher probability of midship and forward strike compared to the IMO data. The IMO tanker probabilities are used in this study.

4. Sensitivity analysis

4.1. Struck ships

Four struck ships are used in the sensitivity analysis. The ships include two 150k dwt oil tankers, one single hull and one double hull, and two 45k dwt oil tankers, one single hull and one double hull. SIMCOL input data for these ships are provided in Tables 4 and 5. Collision scenario pdfs specified in Section 3 are used to develop 10,000 collision cases that are applied to each of these four ships using SIMCOL. SIMCOL calculates damage penetration, damage length and absorbed energy for each of these cases.

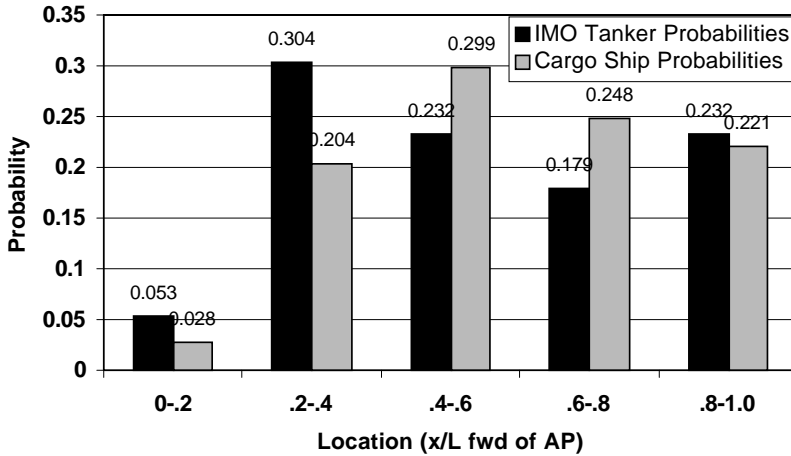


Fig. 14. Longitudinal damage location probabilities.

Table 4
Struck ship principal characteristics

| | DH150 | SH150 | DH45 | SH45 |
|--------------------------|--------|--------|-------|-------|
| Displacement (MT) | 151861 | 152395 | 47448 | 47547 |
| Length (m) | 261.0 | 266.3 | 190.5 | 201.2 |
| Breadth (m) | 50.0 | 50 | 29.26 | 27.4 |
| Depth (m) | 25.1 | 25.1 | 15.24 | 14.3 |
| Draft (m) | 16.76 | 16.76 | 10.58 | 10.6 |
| Double bottom height (m) | 3.34 | NA | 2.1 | NA |
| Double hull width (m) | 3.34 | NA | 2.438 | NA |

4.2. Results and discussion

Figs. 15 and 16 are the resulting distributions for damage penetration and damage length. Table 6 lists mean values for scenario variables, damage penetration, and damage length. The damage pdfs for the four struck ships are quite similar. Unlike the IMO standard pdfs, penetration in these pdfs is not normalized with breadth. The larger struck ships must absorb more energy due to their higher inertia, but structural scantlings are also larger so damage penetrations and lengths for the 150k dwt ships are similar to the 45k dwt ships. Comparing the mean values in Table 6, on the average, the single hull ships do have larger penetrations and damage lengths than the double hull ships, and the larger ships have larger penetrations and damage lengths than the smaller ships.

In order to assess the sensitivity of damage penetration and length to the collision scenario variables, a second order polynomial response surface is fit to the 10,000 cases of SIMCOL results for each ship. Figs. 17–22 provide the results of this

Table 5
Stuck ship structural characteristics

| | DH150 | SH150 | DH45 | SH45 |
|-------------------------------------|-------|-------|-------|------|
| Web frame spacing (mm) | 5.2 | 5.2 | 3.505 | 3.89 |
| Smeared deck thickness (mm) | 29.4 | 28.2 | 27.6 | 30.5 |
| Smeared inner bottom thickness (mm) | 37.1 | NA | 27.8 | NA |
| Smeared bottom thickness (mm) | 36.6 | 44.2 | 34 | 38.5 |
| Smeared stringer thickness (mm) | 14.9 | NA | NA | NA |
| Smeared side shell thickness (mm) | 26.7 | 27.8 | 24.5 | 23.6 |
| Smeared inner side thickness (mm) | 28.1 | NA | 20.1 | NA |
| Smeared long bhd thickness (mm) | 25.1 | 24.5 | 20 | 33.4 |
| Smeared upper web thickness | 12.5 | 12.5 | 12.7 | 19 |
| Smeared lower web thickness | 14.5 | 16 | 12.7 | 19 |

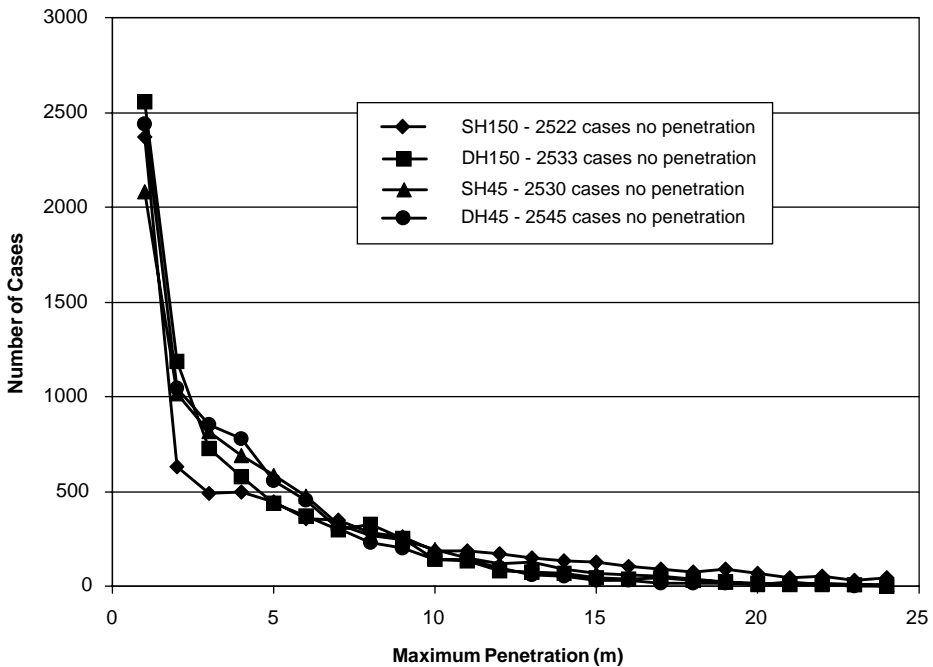


Fig. 15. Damage penetration distribution given penetration.

analysis. In each of the figures, the other collision scenario variables are assigned the mean values listed in Table 6.

Fig. 17 shows a very significant increase in damage penetration as a function of striking ship displacement with diminishing increases above 40k ton. The variation with strike location (Fig. 18) is much less with smaller penetrations for strikes away from midships where more striking energy is converted to struck ship yaw. Fig. 19

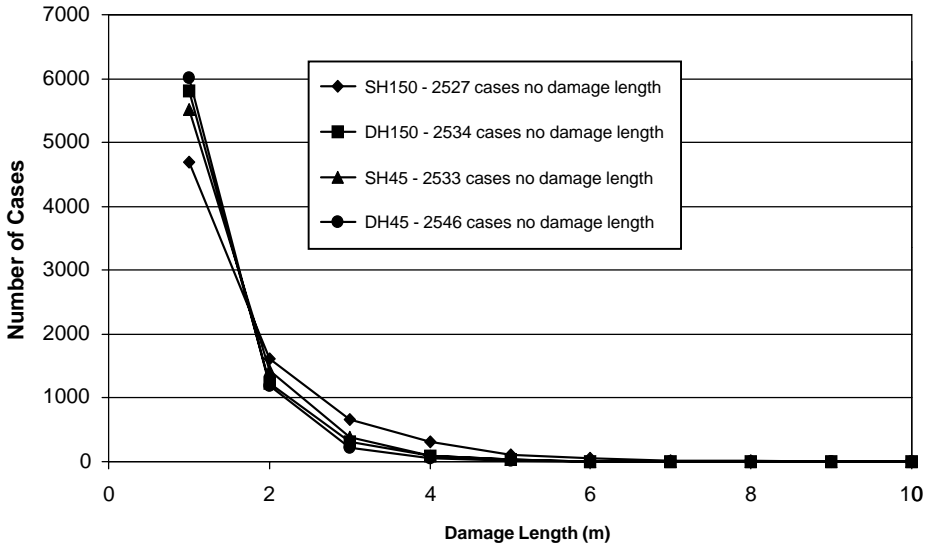


Fig. 16. Damage length distribution.

Table 6
Mean scenario and damage values

| | All | DH150 | SH150 | DH45 | SH45 |
|---------------------------------------|----------|-------|-------|-------|-------|
| Mean struck ship velocity (knots) | 2.49 | | | | |
| Mean striking ship velocity (knots) | 4.27 | | | | |
| Mean strike location (x/L) | 0.47 | | | | |
| Mean collision angle | 90.00 | | | | |
| Mean striking ship displacement (ton) | 13660.00 | | | | |
| Mean damage penetration (m) | | 1.385 | 2.28 | 1.281 | 1.571 |
| Mean damage length (m) | | 2.523 | 3.87 | 2.291 | 2.809 |

shows penetration is very sensitive to striking ship speed over the full range of speeds considered. Fig. 20 shows that penetration is also very sensitive to collision angle with maximum penetration occurring at 80–85° (from the bow) where kinetic energy from both striking and struck ships combine to maximize penetration. Collision angles below approximately 25° and above 150° result in glancing blows that do not penetrate. Fig. 22 shows damage lengths are largest for collision angles of approximately 75°. Fig. 22 shows penetration is less sensitive to struck ship speed.

5. Absorbed energy

A potential simplification for the collision scenario definition requires that the external ship dynamics problem be solved uncoupled from the internal deformation

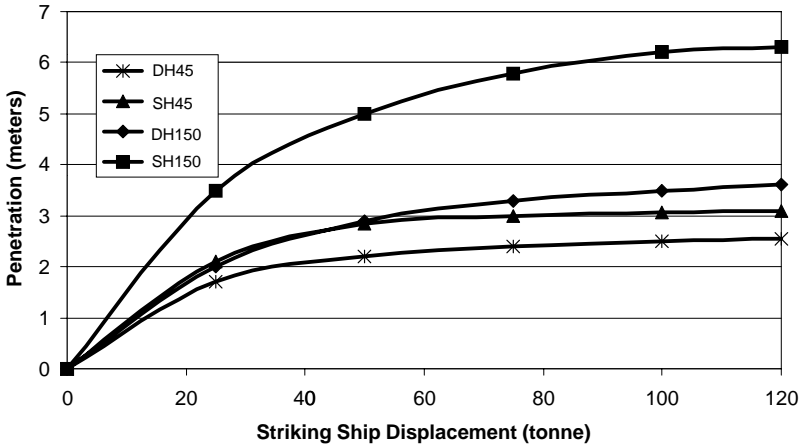


Fig. 17. Penetration versus striking ship displacement.

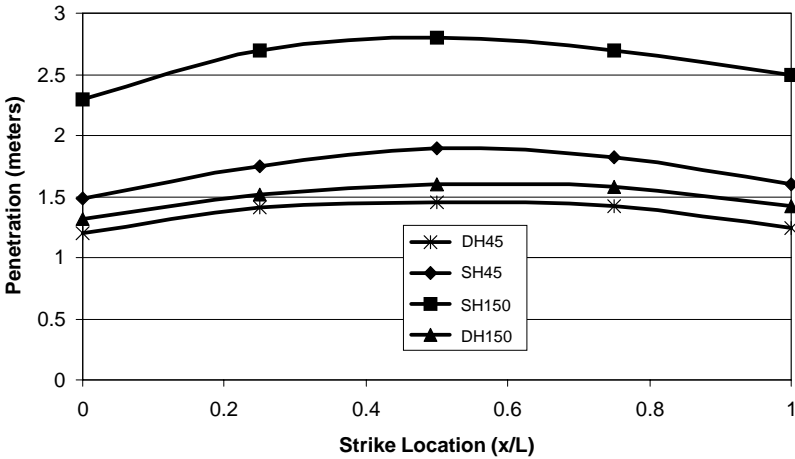


Fig. 18. Penetration versus strike location.

problem. This allows multiple collision scenario random variable definitions to be replaced by pdfs for transverse and longitudinal absorbed energy only. This section examines the validity of this simplification.

5.1. Absorbed energy calculation

Pedersen and Zhang [19] derive expressions for absorbed energy uncoupled from internal mechanics. Collision absorbed energies in the ζ (transverse) direction and η

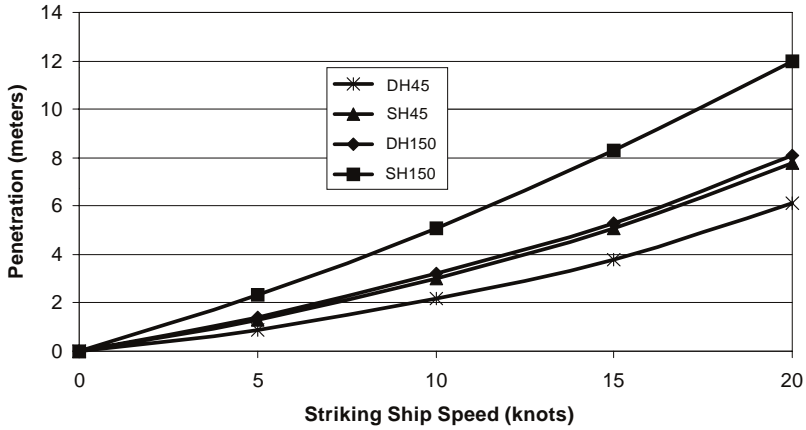


Fig. 19. Penetration versus striking ship speed.

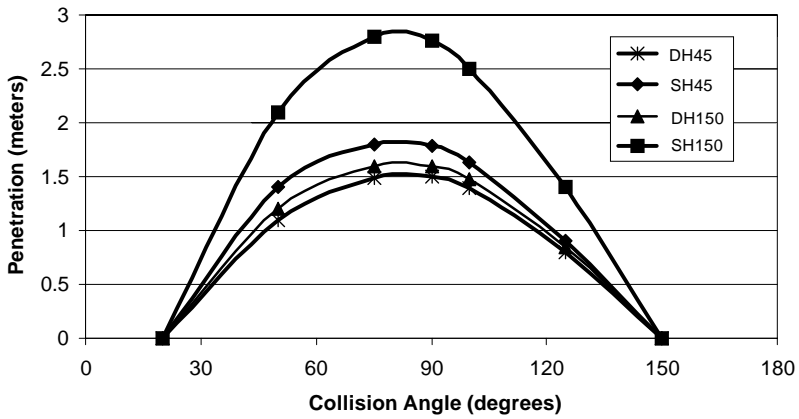


Fig. 20. Penetration versus collision angle.

(longitudinal) direction are:

$$\begin{aligned}
 E_{\xi} &= \int_0^{\xi_{\max}} F_{\xi} d\xi = \frac{1}{2} \frac{1}{D_{\xi} + \mu D_{\eta}} \xi(0)^2, \\
 E_{\eta} &= \int_0^{\eta_{\max}} F_{\eta} d\eta = \frac{1}{2} \frac{1}{1/\mu K_{\xi} + K_{\eta}} \eta(0)^2, \\
 E_{\text{total}} &= E_{\xi} + E_{\eta},
 \end{aligned}
 \tag{31}$$

where the coefficients D_{ξ} , D_{η} , K_{ξ} , K_{η} are algebraic expressions that are a function of the ship masses, strike location, collision angle, and added mass coefficients. Assumed added mass coefficients are 0.05 in surge, 0.85 in sway and 0.21 in yaw.

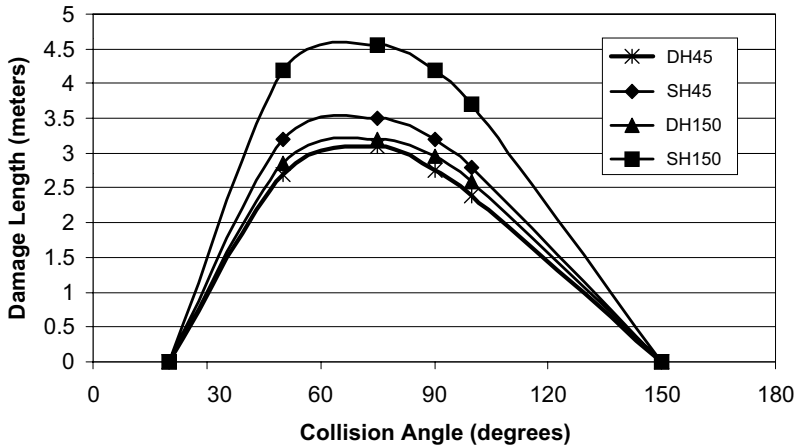


Fig. 21. Damage length versus collision angle.

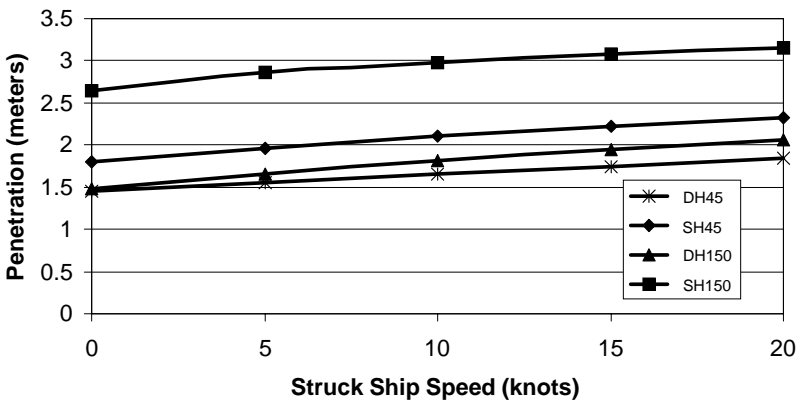


Fig. 22. Penetration versus struck ship speed.

These values correspond with an intermediate collision-impact duration. $\eta \dot{0}$ and $\xi \dot{0}$ are the relative longitudinal and transverse velocities between the two ships just prior to impact. Eq. (30) assumes that the two ships stick together on impact. Whether the two ships slide or stick is determined by the ratio of transverse to longitudinal force impulses at impact. If this ratio exceeds the coefficient of static friction, it is assumed that the two ships slide. The impulse ratio at impact is assumed to be constant for the entire process.

Absorbed energy in SIMCOL is calculated by multiplying transverse force by transverse displacement and longitudinal force by longitudinal displacement for each time step, and then summing for all time steps until the end of the collision event. The relationship between longitudinal and transverse forces is very dependent on the internal deformation of the structure and their relationship varies from time step to time step as the struck ship is penetrated.

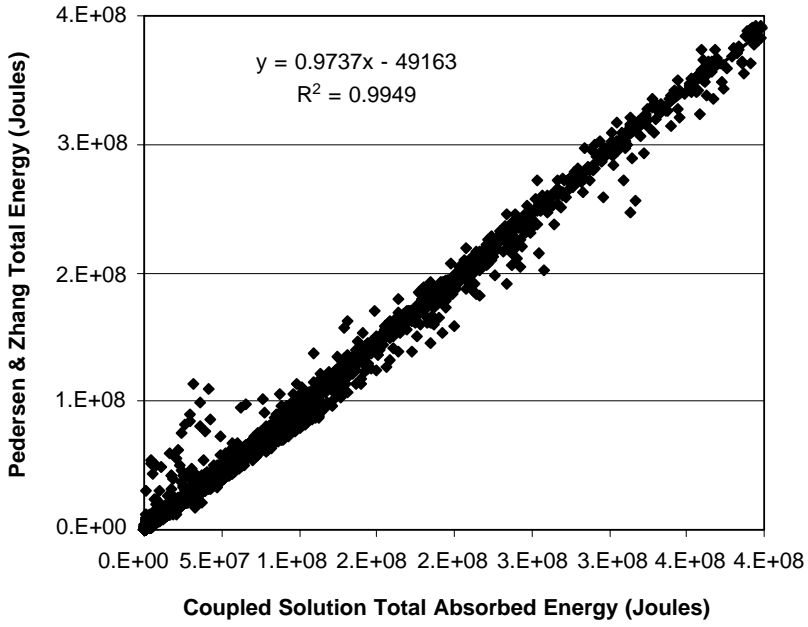


Fig. 23. Total absorbed energy.

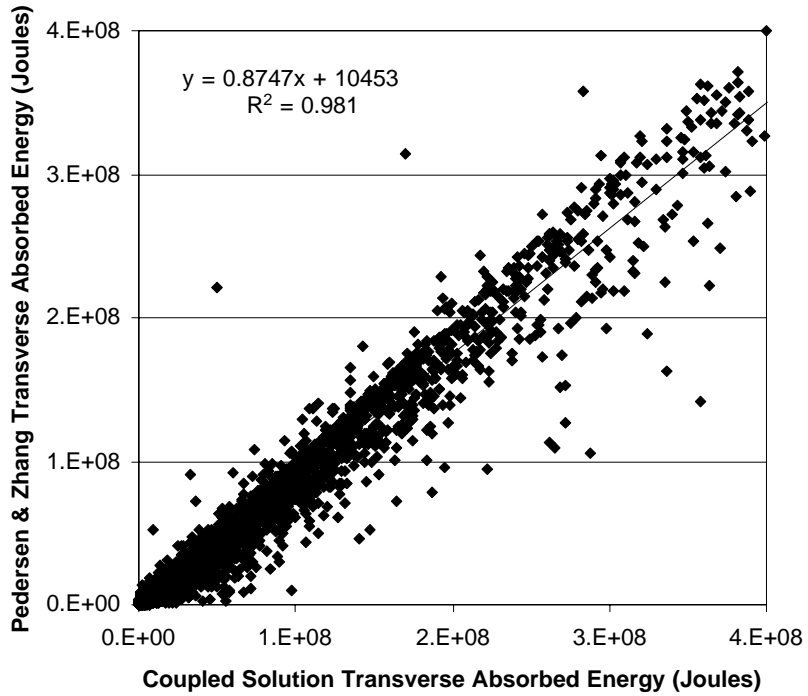


Fig. 24. Transverse absorbed energy.

5.2. Absorbed energy results and discussion

Figs. 23–25 compare absorbed energy calculated using the Pedersen and Zhang method to energy calculated using SIMCOL. Total absorbed energy shown in Fig. 23 is very similar in the two cases, particularly considering the significant difference in the two methods. The longitudinal and transverse components show a larger difference, particularly in the longitudinal direction. This may result from differences in structural resistance in the transverse and longitudinal directions, which in SIMCOL varies during the collision process. The difference in longitudinal absorbed energy is potentially significant because once the structure is penetrated, longitudinal damage extent determines the number of compartments that are opened to the sea. This has a significant effect on damage stability and oil outflow.

6. Conclusions and recommendations

An accurate definition of collision scenario random variables is essential for predicting collision damage penetration and length. Probabilistic damage extents are

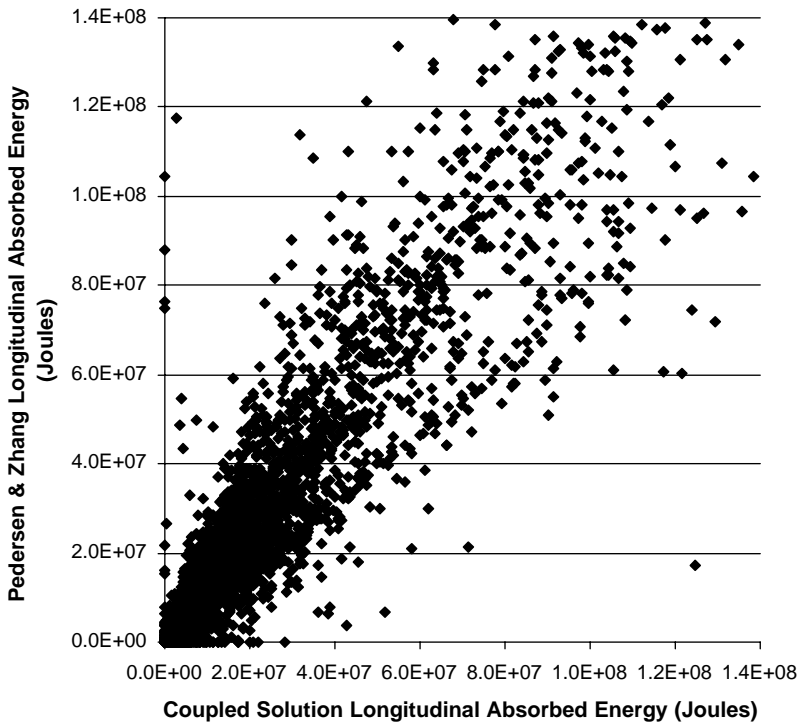


Fig. 25. Longitudinal absorbed energy.

very sensitive to striking ship displacement, striking ship speed and collision angle. A significant effort is warranted to insure that pdfs for these random variables are correct. Damage extents are less sensitive to struck ship speed and strike location.

When estimating damage stability and oil outflow, damage length is a very important factor. Using uncoupled methods to predict absorbed longitudinal energy may not provide sufficient accuracy for this calculation.

Normalization of damage extents using struck ship principal characteristics (L , B , D) as in the standard IMO pdfs may not be a reasonable approach over the full range of collision scenarios. This requires further investigation.

Future work will investigate the sensitivity of probabilistic damage extents to struck ship structural scantlings and will consider striking ship bow deformation.

References

- [1] Sirkar J, et al. A framework for assessing the environmental performance of tankers in accidental groundings and collisions. *SNAME Trans* 1997;105:253–95.
- [2] Crake K. Probabilistic evaluations of tanker ship damage in grounding events. Naval Engineer Thesis, Department of Ocean Engineering, MIT, 1995.
- [3] Rawson C, Crake K, Brown AJ. Assessing the environmental performance of tankers in accidental grounding and collision. *SNAME Trans* 1998;106:41–58.
- [4] Chen D. Simplified Collision Model (SIMCOL). Master of Science Thesis, Department of Ocean Engineering, Virginia Tech, 2000.
- [5] Brown AJ, et al. Structural design and response in collision and grounding. *SNAME Trans* 2000;108:447–73.
- [6] Brown AJ, Amrozowicz M. Tanker environmental risk—putting the pieces together. *SNAME/SNAJ International Conference on Designs and Methodologies for Collision and Grounding Protection of Ships*, 1996.
- [7] Hutchison BL. Barge collisions, rammings and groundings—an engineering assessment of the potential for damage to radioactive material transport casks. Report No. SAND85-7165 TTC-05212, 1986.
- [8] Rosenblatt & Son, Inc. Tanker structural analysis for minor collision. USCG Report, CG-D-72-76, 1975.
- [9] McDermott JF, et al. Tanker structural analysis for minor collisions. *SNAME Trans* 1974;82: 382–414.
- [10] Minorsky VV. An analysis of ship collisions with reference to protection of nuclear power plants. *J Ship Res*, 1959.
- [11] Reardon P, Sprung JL. Validation of Minorsky's ship collision model and use of the model to estimate the probability of damaging a radioactive material transportation cask during a ship collision. Proceedings of the International Conference on Design and Methodologies for Collision and Grounding Protection of Ships, San Francisco, 1996.
- [12] Sandia National Laboratories. Data and methods for the assessment of the risks associated with the maritime transport of radioactive materials results of the Searam program studies. Report SAND98-1171/2, Albuquerque, NM, 1998.
- [13] Lloyds. Lloyds Worldwide Ship data. Provided by MARAD, 1993.
- [14] ORI. Hazardous environment experienced by radioactive material packages transported by water. Silver Spring, MD, 1980.
- [15] ORI. Accident severities experienced by radioactive material packages transported by water. Silver Spring, MD, 1981.
- [16] USCG Ship Casualty Data, 1982–1990.

- [17] IMO. Interim guidelines for approval of alternative methods of design, construction of oil tankers. Under Regulation 13F(5) of Annex I of MARPOL 73/78, Resolution MEPC 66 (37), 1995.
- [18] IMO. Comparative study on oil tanker design. Distribution of actual penetrations and damage locations along ship's length for collisions and groundings. IMO paper, MEPC 32/7/15, Annex 5, 1989.
- [19] Pedersen PT, Zhang S. On impact mechanics in ship collisions. *Marine Struct* 1998;11:429–49.